Chapter

Photoanode Applications of Polyene-Diphenylaniline Dyes Molecules Adsorbed on TiO_2 Brookite Cluster

Ife Elegbeleye, Eric Maluta, Regina Maphanga, Michael Walter and Oliver Brügner

Abstract

TiO_2 has excellent photoelectrochemical properties, which makes its suitable for photoanode applications. TiO_2 is widely utilized as semiconductor for dye-sensitized photoanode owing to its excellent stability and availability. The brookite polymorph of TiO_2 has been suggested to demonstrate better photocatalytic properties. In this work, we studied the adsorption of polyenediphenyl-aniline dyes on $(TiO_2)_{n = 8, 68}$ brookite clusters using density functional theory (DFT). We report our results on the UV–Vis absorption spectra of the dyes and dyes adsorbed on TiO_2 clusters, adsorption energies of the dyes adsorbed on TiO_2 clusters, electronic density of states and projected electronic density of states of the dyes adsorbed on TiO_2 complex, and electron density of the main molecular orbitals involved in photoexcitation for dye-sensitized solar cells application. The calculated adsorption energies of D5@$(TiO_2)_{68}$, D7@$(TiO_2)_{68}$, D9@$(TiO_2)_{68}$, and D11@$(TiO_2)_{68}$ are 4.84, 4.78, 4.66 and 4.92 eV, respectively. The results of the adsorption energies are in the order D11@$(TiO_2)_8$ > D9@$(TiO_2)_8$ > D7@$(TiO_2)_8$ > D5@$(TiO_2)_8$ and D11@ $(TiO_2)_{68}$ > D5@ $(TiO_2)_{68}$ > D7@ $(TiO_2)_{68}$ > D9@ $(TiO_2)_{68}$. This implies that D11 dye molecule reacts more strongly with $(TiO_2)_8$ and $(TiO_2)_{68}$ brookite clusters than the other corresponding dye molecules.

Keywords: dye sensitized solar cells, TiO_2 brookite semiconductor, polyene-diphenyl-aniline dyes, density functional theory, optical properties

1. Introduction

The fascinating features of dye sensitized solar cells (DSSC) over conventional solar energy devices are their low manufacturing temperature, low fabrication cost, flexibility, and potential of high photon to current conversion efficiency [1–3]. DSSC photoanode is made up of dye molecules chelated to typical TiO_2 semiconductors surface. TiO_2 is widely used as semiconductor for DSSCs because it is readily available

and has good stability when illuminated to sunlight [4, 5]. The ruthenium N3 complex has been extensively utilized in TiO_2-DSSCs architecture, reported to achieve 11–12% power conversion efficiency (PCE) [6–7]. However, these ruthenium dye complexes are relatively expensive, toxic, and require difficult synthetic and refinement processes. On the other hand, organic dyes have advantages of non-toxicity, low cost, and availability of raw materials and are environmentally friendly, which makes them more desirable than the ruthenium complexes [3, 8].

Polyenediphenyl-aniline dye (on TiO_2 semiconductor) based on ionic liquid electrolyte and iodide/triiodide has been reported as a promising candidate for DSSC applications with PCE of 6.5 and 5% [9, 10]. TiO_2 exists in three major polymorphs, namely, anatase, rutile, and brookite [4]. Anatase is mainly synthesized from TiO_2 powder by sol-gel method, while rutile can be obtained as a by-product of precipitation at low temperature in an acidic medium [1, 11]. Synthesizing pure brookite is challenging owing to the intergrowth morphology of anatase and rutile usually encountered during the synthetic process [12–14]. As a result of this difficult synthetic route, most of the studies on TiO_2 polymorphs are centered on anatase and rutile phases as prototypical models for DSSCs fabrication [15, 16]. There are very few studies on the photocatalytic properties of TiO_2 brookite. However, some recent studies have suggested that brookite may exhibit fascinating photocatalytic properties and may perform better as a semiconductor than the typically used anatase [17–21]. Zallen et al. reported on the optical absorption edge of brookite TiO_2 at room temperature using natural crystals [16]. The photon energy spanning from 2.1 to 3.54 eV, absorption coefficient of 2000 cm^{-1}, and optical gap of 1.9 eV were reported for brookite crystals. The absorption edge of brookite was observed to be broad and extends to the solar spectrum visible region, whereas steep edges were observed for rutile and anatase polymorphs of TiO_2 in the visible region [16]. The crystallographic description of brookite polymorphs is presented in **Table 1**.

Brookite has an orthorhombic crystalline structure with eight formula units in the orthorhombic cell; its unit cell is described by the space group *Pbca* [4]. Brookite formation may be envisioned as the joining of TiO_6 distorted octahedral sharing three edges, each with a titanium atom at its center and oxygen atoms at its corners.

Information about the interfacial reaction of TiO_2 brookite with the promising polyenediphenylaniline organic dye is crucial for the understanding and optimization of photo conversion function, light harvesting, and photocurrent densities in DSSCs.

In this study, we carried out density functional theory (DFT) and time-dependent DFT (TD-DFT) study on the adsorption of polyenediphenyl-aniline dyes on TiO_2 brookite in order to understand the interaction between TiO_2 brookite and

	Lattice parameter (Å)	Space group	System type	Energy bandgap (eV)
Rutile	a = 4.594 c = 2.958	$P4_2/mnm - D_{4h}^{14}$	Tetragonal	3.0
Anatase	a = 3.784 c = 9:515	$I4_1amd - D_{4h}^{19}$	Tetragonal	3.4
Brookite	a = 9.166 b = 5.436 c = 5.135	$Pbca - D_{2h}^{15}$	Orthorhombic	3.3

Table 1.
Properties of rutile, brookite, and anatase polymorphs of TiO_2 [4].

polyenediphenylaniline dyes. We report on the optical and electronic properties of the polyenediphenyl-aniline dyes and the dyes adsorbed on TiO_2 brookite clusters.

2. Materials and methods

The main part of density-functional theory calculations was performed within an atomic simulation environment (ASE) [22] and the GPAW package [23, 24]. GPAW implements the projector-augmented wave method with the smooth wave-functions and electron density represented on real space grids [21]. The exchange correlation energy was approximated within the generalized gradient approximation PBE [25]. The structures were relaxed without any symmetry constraints until all forces were found to be below 0.05 eV/Å. Their structure was visualized with Avogadro [26]. Optical spectra were obtained from linear response time-dependent DFT [27, 28].

The structures of the D5, D7, D9, and D11 dye molecules [10] were built in Gaussian 03 quantum chemical package [25, 29]. First geometrical optimization of the dye molecules was performed while employing the density functional theory and hybrid density functional theory B3LYP and 6-31G* basis set [30, 31] with the default integration grid as implemented in Gaussian 03. The structures were subsequently relaxed as described above and are depicted in **Figure 1(a-d)**.

The TiO_2 brookite models considered in this study are presented in **Figure 2**. The cluster models were imported using the crystallographic information mode (cif) from CASTEP material studio [32]. The brookite cluster models are brookite $(TiO_2)_8$ comprising eight titanium and 16 oxygen atoms, while brookite $(TiO_2)_{68}$ is a periodic supercell comprising 68 titanium atoms and 136 oxygen atoms [21]. The periodic structure is a bulk structure comprising unit cells that are repeated in x and y direction to form a cluster or supercell of an arbitrary size.

All the structures of the dye@TiO_2 were relaxed in vacuum using the PBE exchange correlation functional [32]. The structures were considered to have converged when the maximum forces that were acting on all the atoms were lower than 0.05 eV/Å. The periodic boundary conditions were implemented during the relaxation and the atoms of the cluster. The cluster were reoriented during the relaxation until the ground state structure was obtained where they become stable, and the forces converge to a value of 0.05 eV/Å.

The polyenediphenyl aniline dye molecules were adsorbed unto the TiO_2 surface *via* the carboxylic group in the bidentate bridging (BB) adsorption mode [33, 34], in which each of the oxygen atoms of the carboxylic moiety binds to titanium atom on the TiO_2 clusters. This mode was adopted because it was reported to be more energetically favorable [33, 34]. The adsorption energies and optical and electronic properties of the dye molecules absorbed on TiO_2 cluster were calculated upon adsorption.

2.1 Structures of polyenediphenyl-aniline dyes absorbed on (TiO2) n = 8, 68

Four polyenediphenyl-aniline dye molecules coded D5, D7, D9, and D11 were separately adsorbed by bidentate adsorption mode on TiO_2 clusters with stoichiometry $(TiO_2)_8$ and $(TiO_2)_{68}$ as showed in **Figures 3(a-d)** and **4(a-d)**. All dye@TiO_2 complexes were relaxed upon adsorption; the relaxed structures of the dye molecules adsorbed on $(TiO_2)_8$ and $(TiO_2)_{68}$ clusters are presented in **Figures 3** and **4**, respectively. Bidentate bridging adsorption mode was utilized to adsorb the polyenediphenyl-aniline dye molecules on the TiO_2 clusters *via* the carboxylic acid moiety. Each of

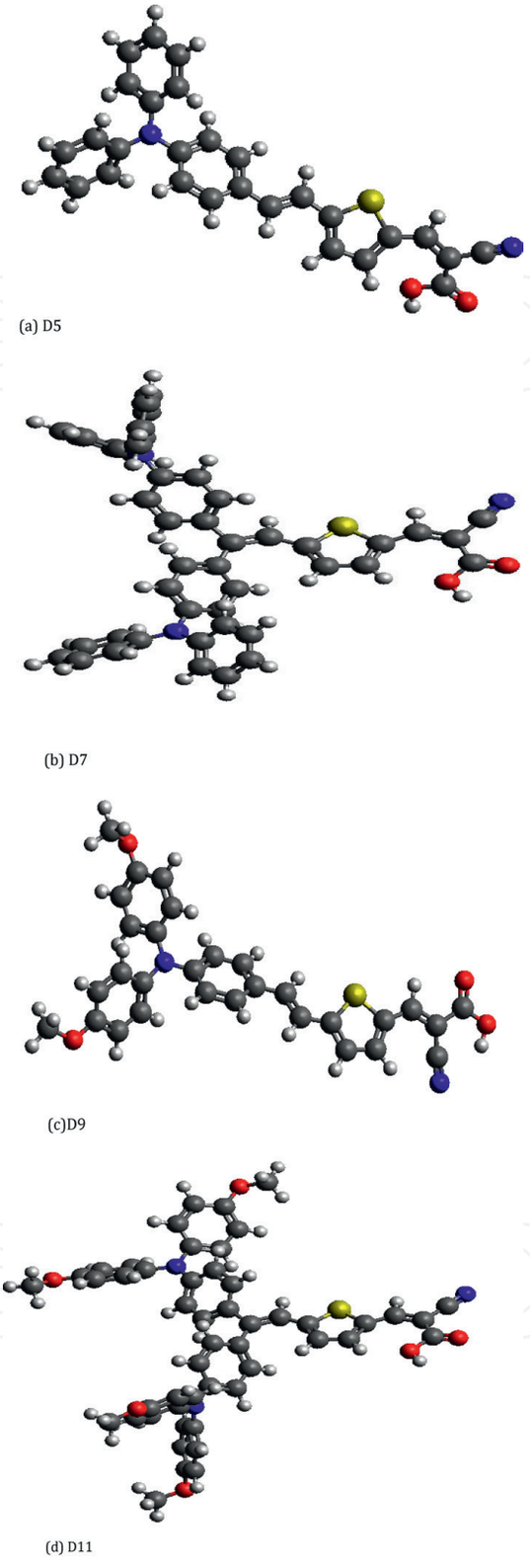

Figure 1.
Structures of the polyenediphenyl-aniline dye molecules in gas-phase.

the two oxygen atoms was adhered to the titanium atom on the TiO_2 cluster surface. In order to achieve a stable system for TD-DFT calculations, the atom of the hydrogen was transferred to a neighboring oxygen atom.

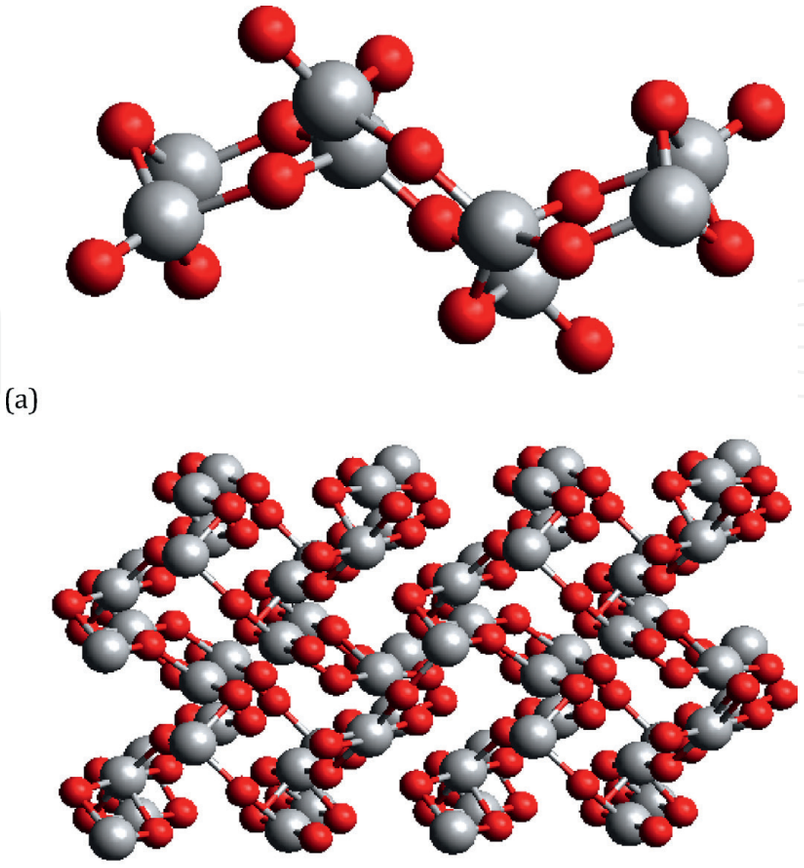

(a)

(b)

Figure 2.
(a-b) Broookite $(TiO_2)_{n = 8, 68}$ cluster periodic models considered for dye molecule adsorption in this study.

2.2 Adsorption energies of polyene-diphenylaniline dye molecules absorbed on $(TiO2)_{n = 8, 68}$ brookite clusters

The relaxation energies of the dye molecules, $(TiO_2)_8$ and $(TiO_2)_{68}$ brookite clusters, and polyenediphenyl-aniline dyes-TiO_2 complexes were computed the adsorption energies using (Eq. (1)).

$$E_{ads} = \left[E_{TiO_2} + E_{(\text{molecule})} \right] - \left[E_{(TiO_2 + \text{molecule})} \right] \quad (1)$$

where E_{TiO_2} is the energy of the TiO_2 complex, $E_{molecule}$ is the energy of the adsorbate, and $E_{(TiO_2 + \text{molecule})}$ is the total energy of the TiO_2 with the adsorbed molecule. The adsorption energy denotes the binding ability of the dye molecules [5, 21, 33, 35–37]. The adsorption energies of D5, D7, D9, and D11 dyes adsorbed on $(TiO_2)_8$ and $(TiO_2)_{68}$ clusters are listed in **Table 2**. All the calculated results show a positive adsorption energy, suggesting stable grafting of the dyes molecules unto the surface of TiO_2. The calculated adsorption energies of D5@$(TiO_2)_8$, D7@$(TiO_2)_8$, D9@$(TiO_2)_8$, and D11@ $(TiO_2)_8$ are 1.60, 1.62, 1.67, and 1.81 eV, respectively. The order of the adsorption energies is D11@$(TiO_2)_8$ > D9@$(TiO_2)_8$ > D7@$(TiO_2)_8$ > D5@$(TiO_2)_8$. The findings suggest that D11 dye molecule exhibits

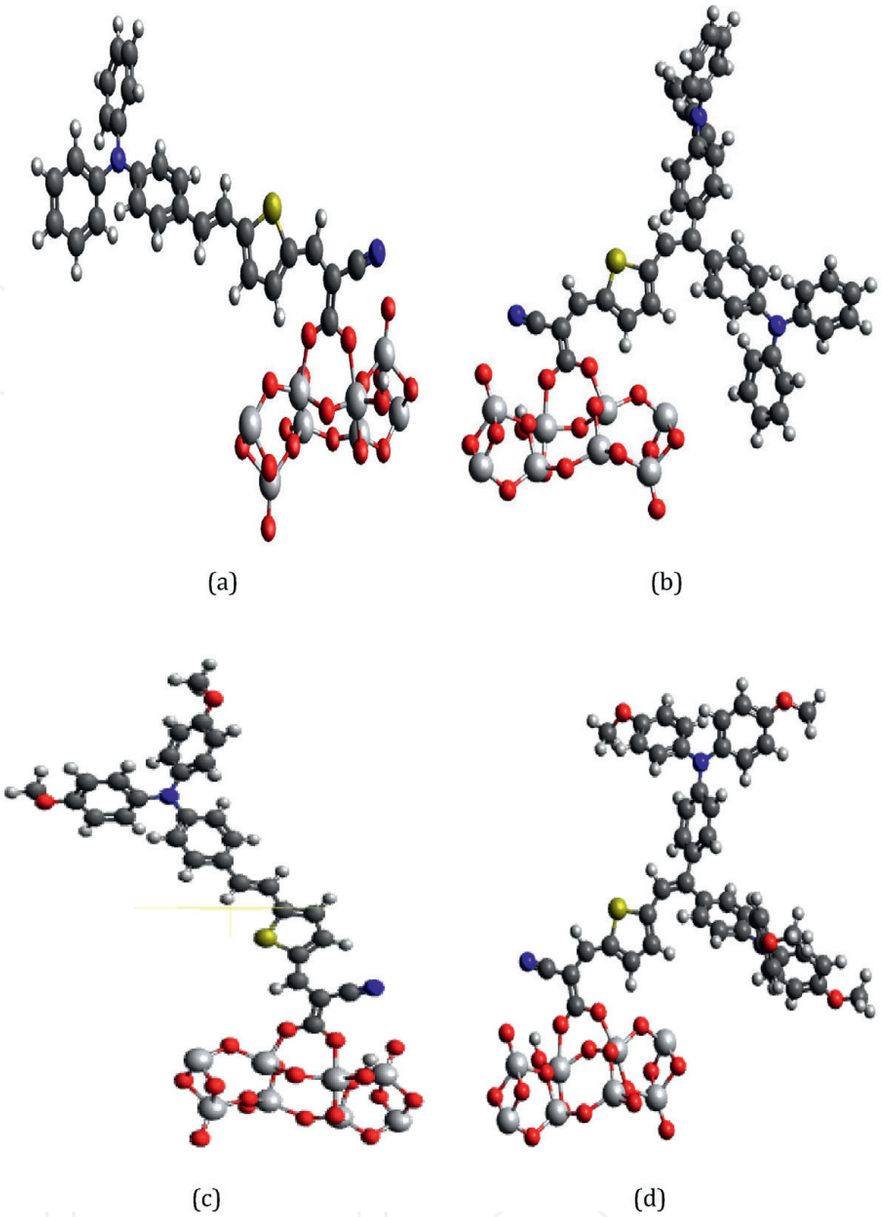

Figure 3.
Structures of polyenediphenyl-aniline dyes absorbed on $(TiO_2)_8$ (a) D5@$(TiO_2)_8$, (b) D7@$(TiO_2)_8$, (c) D9@$(TiO_2)_8$, and (d) D11@$(TiO_2)_8$. Gray spheres represent titanium atoms; red spheres represent oxygen atoms; white spheres represent hydrogen atoms; yellow spheres represent sulfur atoms; dark gray balls represent carbon atoms, and blue spheres represent nitrogen atoms.

stronger reaction with $(TiO_2)_8$ brookite cluster than the other dye molecules. Values of 4.84, 4.78, 4.66, and 4.92 eV were obtained for the adsorption energies of D5@$(TiO_2)_{68}$, D7@ $(TiO_2)_{68}$, D9@ $(TiO_2)_{68}$, and D11@ $(TiO_2)_{68}$, respectively. Unlike $(TiO_2)_8$, the order of the adsorption energies is not sequential but D11@$(TiO_2)_{68}$ > D5@$(TiO_2)_{68}$ > D7@$(TiO_2)_{68}$ > D9@$(TiO_2)_{68}$. The results show that D11 dye molecule demonstrates a stronger reaction with $(TiO_2)_{68}$ brookite surface than D5, D7, and D9 molecules. Variation in the obtained adsorption energies for the four dye molecules adsorbed on the different brookite surfaces indicates that the cluster size affects the binding ability of the molecules. The polyenediphenyl-aniline dye molecules are found to have stronger interaction with the $(TiO_2)_{68}$ cluster than $(TiO_2)_8$ cluster.

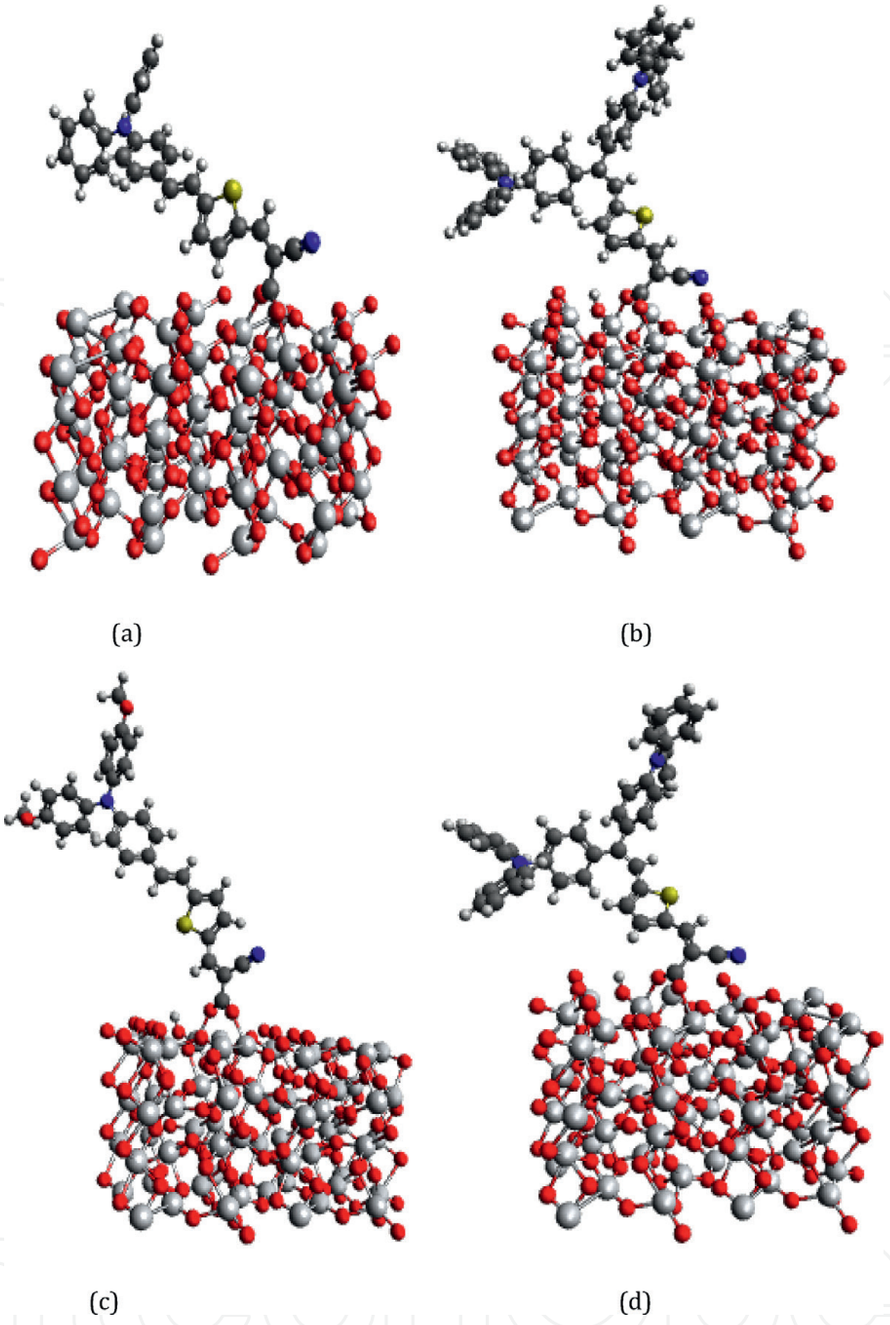

Figure 4.
Structures of polyenediphenyl-aniline dyes absorbed on $(TiO_2)_{68}$ (a) D5@$(TiO_2)_{68}$, (b) D7@$(TiO_2)_{68}$, (c) D9@$(TiO_2)_{68}$, and (d) D11@$(TiO_2)_{68}$. Same notation as in **Figure 4**.

Adsorption Energy of Dyes@$(TiO_2)_{n\ =\ 8,68}$		**(eV)**
Dyes@$(TiO_2)_8$	D5@$(TiO_2)_8$ D7@$(TiO_2)_8$ D9@$(TiO_2)_8$ D11@$(TiO_2)_8$	1.60 1.62 1.67 1.81
Dyes@$(TiO_2)_{68}$	D5@$(TiO_2)_{68}$ D7@$(TiO_2)_{68}$ D9@$(TiO_2)_{68}$ D11@$(TiO_2)_{68}$	4.84 4.78 4.66 4.93

Table 2.
Adsorption energies of dyes @ $(TiO_2)_{n\ =\ 8,\ 68}$ clusters.

Balaganapathi et al. synthesized porous brookite and mixed brookite with rutile TiO_2 crystals using Polyethylene Glycol (PEG) assisted sol-gel synthesis and investigated their dye adsorption characteristics [38]. Reflectance measurements were used

to determine the optical bandgap of both the brookite and brookite mixed with rutile samples as 2.26 and 2.48 eV, respectively. The reported binding energies ranged from 445 to 470 eV for pure brookite and from 520 to 540 eV for brookite mixed with rutile phase. In this work, the calculated bandgap of brookite was found to be 2.26 eV, which is consistent with the aforementioned study [38].

In another study, Corneliu et al. investigated the adsorption of coumarin dyes C343 on $Ti_nO_{2n+2}H_4$ (n = 14, 24) clusters using DFT/B3LYP with 3-21G (d) or LANL2DZ basis set in vacuum. The reported adsorption energies ranged between 0.429 and 3.254 eV. The findings concluded that the size of the cluster affects adsorption properties and revealed that adsorption onto n = 14 cluster leads to a significant distortion of the cluster and the molecule, a behavior that was not observed with a larger cluster of n = 24. This is in line with our findings and may be the reason why polyenediphenyl-aniline dye molecules are found to absorb more onto $(TiO_2)_{68}$ cluster than $(TiO_2)_8$ cluster [39].

2.3 Optical spectrum of polyenediphenyl-aniline dye molecules adsorbed on brookite $(TiO2)_{n=8,68}$

The excitation spectra of the dyes were calculated in gas phase as shown in **Figure 3**. All the dyes show a region of absorbance between 700 and 900 nm at higher energy region. The two dyes with pure phenyl groups D5 and D7 show two main strong features in their spectrum. The absorption peaks of the D5 dye are located at 450 and 750 nm, while that of D7 dye are located around 480 and 850 nm. D9 shows an absorption peak at 500 and 800 nm, while D11 shows double absorption peaks around 400–500 nm and absorption maximum at 900 nm. The largest absorption wavelength is notable for D11 containing methoxy and polyene groups, which is consistent with the experimental study by Kuang et al. [10], where D11 showed spectral red shifts and thus provided better current-voltage characteristics than the corresponding D5, D7, and D9.

Huy et al. carried out UV/Vis diffuse reflectance spectra measurements of brookite TiO_2/DC668 (styrene-acrylatethin) to infer the optical characteristics and to determine the optical bandgap energy of printed TiO_2 brookite thin film [19]. The study reported that TiO_2/DC668 thin film strongly absorbs light in the UV-A region at wavelength of 379 nm and below, and exhibited absorption between 400 and 700 nm [19]. Their findings is consistent with the near infrared absorption obtained for dye adsorption on brookite in this study.

Polyenediphenyl-aniline dyes D5, D7, D9, and D11 absorption spectra are presented in **Figure 5**. The excited state properties of the dyes bonded to TiO_2 clusters are illustrated by the absorption spectra. The computed UV/Vis spectra of $(TiO_2)_8$ brookite cluster using GPAW/TD-DFT exhibit absorption around 200–400 nm in the UV region. It was observed that polyenediphenly-aniline dye adsorption on $(TiO_2)_8$ brookite cluster results in shifting the absorption peaks to higher wavelength due to photoexcitation. Absorption maxima in the near infrared region were observed to be 750, 850–950, 850, and 950 nm for D5@$(TiO_2)_8$, D7@$(TiO_2)_8$, D9@$(TiO_2)_8$, and D11@$(TiO_2)_8$, respectively. The D11@ $(TiO_2)_8$ complex showed the highest absorption maximum and absorption peak in the near-infrared region. The results revealed that adsorption of polyenediphenly-aniline dye onto $(TiO_2)_8$ cluster improves the spectral responsivity, exhibiting whole spectra range absorption in the UV, visible and near-infrared region of the solar spectrum. This suggests higher photocurrents density in DSSCs.

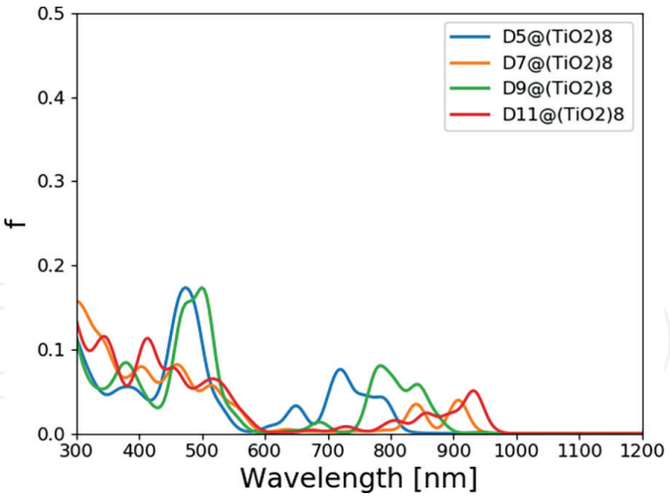

Figure 5.
Optical absorption spectrum of and polyene-diphenylaniline dye molecules adsorbed on $(TiO_2)_8$ cluster.

This makes the complex of this findings consistent with those reported by Huy et al. on a different dye molecule TiO_2/DC668 (styrene-acrylatethin) brookite thin film, exhibiting light absorption in the near-infrared region [19].

2.4 Electronic density of states polyenediphenyl-aniline dye molecules adsorbed on $(TiO2)_{n=8,68}$ brookite clusters

In order to gain further insights into the electronic structure of the dye-TiO_2 complex, GPAW and PBE exchange correction functional was utilized to compute the total density of states (DOS) for D5, D7, D9, and D11 dye molecules absorbed on $(TiO_2)_8$ and $(TiO_2)_{68}$. **Figure 6(a)-(d)** illustrate the total density of states of polyenediphenyl-aniline dye adsorbed onto $(TiO_2)_8$ and $(TiO_2)_{68}$. The DOS is composed of surface valence and conduction bands, separated by a wide bandgap. Upon the adsorption of the dye molecules on TiO_2 clusters, it was observed that sharp molecular energy levels were introduced by the dyes in the wide bandgap of TiO_2 as visible in **Figure 6(a)-(d)**. Thus, adsorption of dye onto the TiO_2 clusters resulted in the introduction of new occupied electronic orbitals in the conduction band and between the two states where there was an initial wide bandgap, thereby reducing the energy bandgap. Also, occupied orbital edge slightly shifted to higher energy levels; the shifting of the two states subsequently results in narrowing of the wide bandgap. This behavior explains the observation on red spectral shift upon dye adsorption discussed in the previous section.

The result of the PDOS for the clusters before the adsorption of the dyes shows that titanium and oxygen atomic orbitals contribute to the valence states; the major contributions of oxygen 2*p* atomic orbitals were mostly to the highest occupied valence band (VB), while the titanium 3*d* atomic orbitals contributions were dominant in the lowest unoccupied state of the conduction band.

Oxygen p atomic orbitals contributions dominated the valence band with minor contributions from *p* atomic orbitals of titanium. The conduction band major contributions emanate from the *d* and *p* orbitals of titanium.

The PDOS spectra of the dyes @$(TiO_2)_8$ and dyes@$(TiO_2)_{68}$ are presented in **Figure 6**. m2*p* orbitals of carbon, 2*p* orbitals of nitrogen, 3*p* orbitals of sulfur, 3*d* orbitals of titanium, and 2*p* orbitals of oxygen contributed majorly to the valence

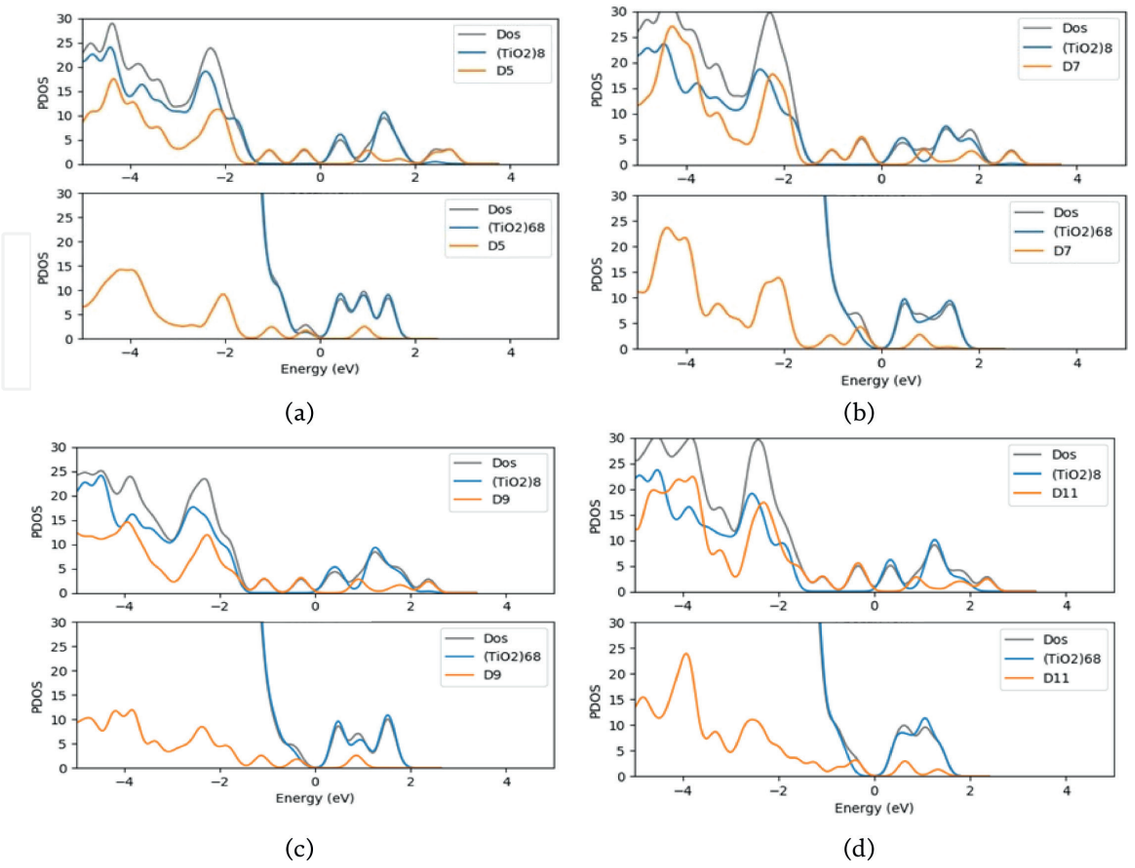

Figure 6.
(a) The total density of states for D5@ $(TiO_2)_8$ and D5@ $(TiO_2)_{68}$ (b) density of states for D7@ $(TiO_2)_8$ and D7@ $(TiO_2)_{68}$ DOS. (c) Total density of states for D9@ $(TiO_2)_8$ and D9@ $(TiO_2)_{68}$. (d) Total density of states for D11@ $(TiO_2)_8$ and D11@ $(TiO_2)_{68}$.

states, while there is a minor contribution of *p* orbitals of sulfur and oxygen to the conduction band.

The major contributions of *p* atomic orbitals of sulfur and oxygen are dominant in the valence band, while carbon and nitrogen *p* atomic orbitals has minor contributions to the valence states. Sulfur 3*p* orbitals contributions dominate the valence states. The dye molecules constitute the main atomic orbital contributing majorly to the valence states. This explains while the electronic densities of the highest occupied molecular orbital were concentrated on the dye molecules.

2.5 HOMO, LUMO isodensity surfaces of polyenediphenyl-aniline dye molecules adsorbed on $(TiO2)_{n = 8, 68}$ brookite nanocluster

The isodensity surfaces of the molecular orbital responsible for photoexcitation were created from cube files gotten from GPAW. The isodensity surfaces were visualized using the Avogadro software. The isodensity surfaces of the main molecular orbital that were responsible for the photoexcitation of the electrons for the adsorbed polyenediphenyl-aniline dyes@$(TiO_2)_8$ and $(TiO_2)_{68}$ brookite clusters are presented in **Figures 7** and **8**, respectively. The results of the highest occupied molecular orbitals (HOMO) clearly reveal the delocalization of the HOMO on the dye molecule. It is majorly located on the donor group constituting the occupied electronic states, while the lowest unoccupied molecular orbitals (LUMO) obtained

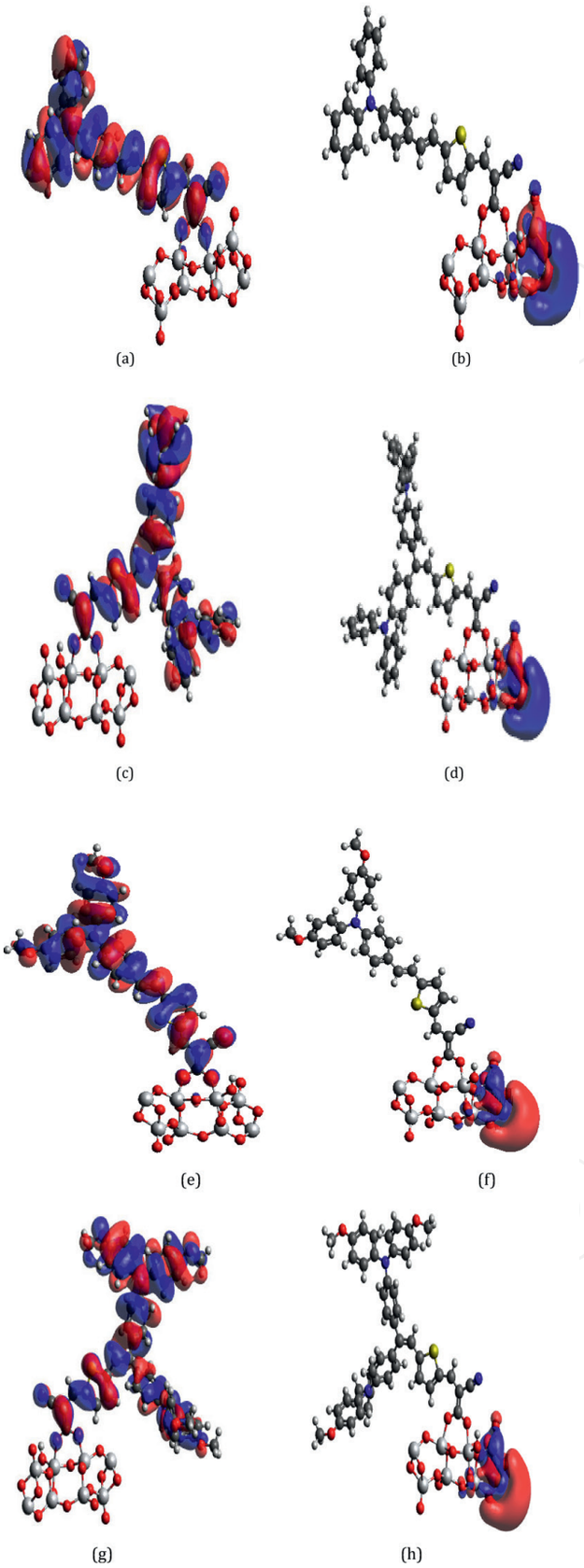

Figure 7.
Isodensity surfaces of molecular orbitals of dyes@ $(TiO_2)_8$ complex (a) D5@ $(TiO_2)_8$ HOMO, (b) D5@ $(TiO_2)_8$ LUMO, (c) D7@ $(TiO_2)_8$ HOMO, (d) D7@ $(TiO_2)_8$ LUMO, (e) D9@ $(TiO_2)_8$ HOMO, (f) D9@ $(TiO_2)_8$ LUMO, (g) D11@ $(TiO_2)_8$ HOMO, and (h) D11@ $(TiO_2)_8$ LUMO.

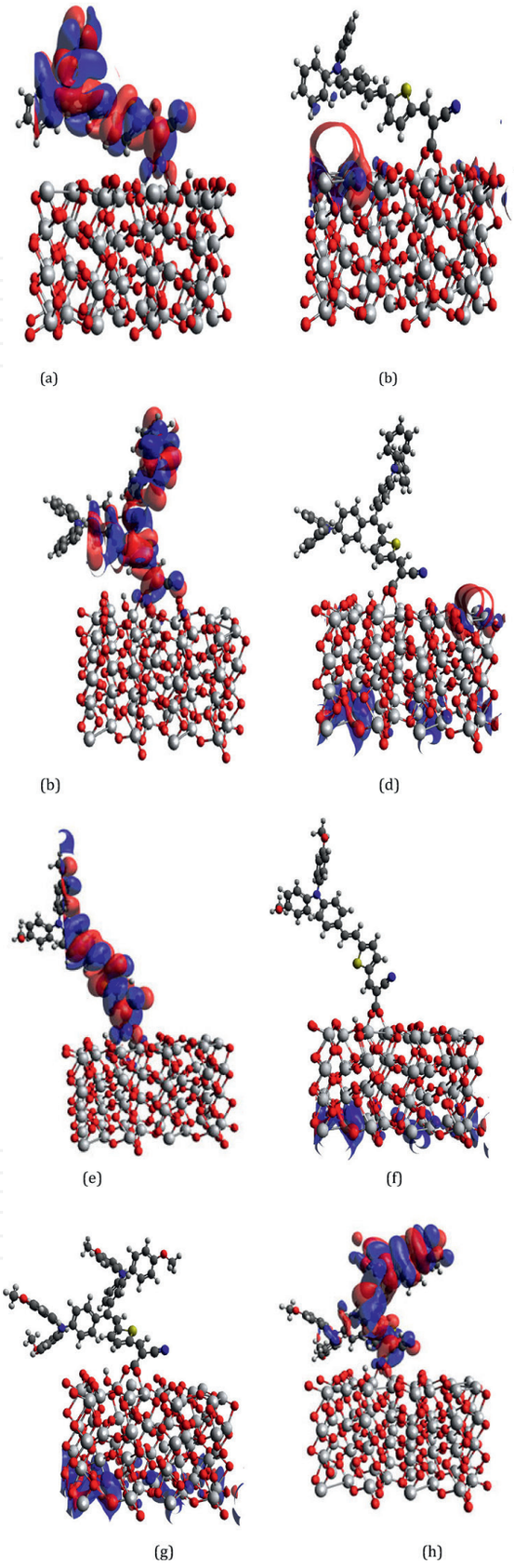

Figure 8.
Isodensity surfaces of molecular orbitals of dyes@(TiO2)68 complex (a) D5@(TiO2)68 HOMO, (b) D5@(TiO2 68 LUMO, (c) D7@(TiO2)68 HOMO, (d) D7@(TiO2)68 LUMO, (e) D9@(TiO2)68 HOMO, (f) D9@(TiO2)68 LUMO, (g) D11@(TiO2)68 HOMO, and (h) D11@(TiO2)68 LUMO.

reveal the concentration on the acceptor group, where the unoccupied electronic states are located. The distributions of the HOMO electron densities on the dye molecule and the distribution of the LUMO electron densities on the TiO_2 brookite indicate that there is a strong interaction between the dye molecules occupied excited state and the conduction band of the TiO_2 brookite semiconductor unoccupied acceptor levels. The concentration of the electronic levels of the HOMO on the dye molecules and the electronic levels of the LUMO on the TiO_2 clusters infer that electrons are injected from excited state of the dye molecules to the conduction band of the TiO_2 semiconductor.

2.6 Energy levels and bandgaps of polyenediphenyl-aniline dye adsorbed on brookite TiO2 complex

The energy levels of the HOMO, LUMO, and the energy gap of polyenediphenyl-aniline dyes, $(TiO_2)_8$, and the dyes adsorbed on $(TiO_2)_8$ clusters are presented in **Table 3**. This is to understand the effect of dye adsorption on the wide bandgap of the brookite TiO_2 clusters. The bandgaps of D5, D7, D9, and D11 polyenediphenyl-aniline dyes are situated at 1.32, 0.98, 1.08, and 0.85 eV, respectively. The lower bandgap values were found for D7 and D11 dyes molecules. To understand the effect of adsorption of the polyenediphenyl-aniline dyes and electron transfer mechanisms from the dye molecules to the TiO_2 semiconductor conduction band upon adsorption, we investigated the bandgap energy levels of the dye absorbed on $(TiO_2)_n$ clusters. The results show that the HOMO of $(TiO_2)_8$ brookite cluster without adsorption was situated at −6.92 eV while the LUMO is at −4.62 eV with a corresponding bandgap of 2.26 eV. It was observed that the adsorption of the dye molecules on $(TiO_2)_8$ brookite cluster introduces new molecular orbital emanating from the dyes into the wide bandgap of the brookite TiO_2 semiconductor cluster, consequently resulting in the narrowing of the bandgap. This new molecular orbital suggests interactions between the dye molecules occupied exited states and the brookite TiO_2 clusters unoccupied acceptor level. The results also suggest the transfer of electron from the dye molecules to the clusters upon adsorption.

3. Conclusions

In this work, we used DFT computational approach to explore the optical and electronic properties of polyenediphenyl-aniline dye adsorbed on TiO_2 brookite clusters for application in DSSCs. The aforementioned dye molecules were absorbed on brookite TiO_2 clusters in order to understand the interfacial properties between brookite TiO_2 semiconductor and the corresponding dye molecules. The adsorption energies, UV/Vis optical absorption properties, HOMO-LUMO energy gap, isodensity surfaces of key molecular orbital, electronic TDOS, and PDOS for various systems were presented and discussed. The presented results were based on polyenediphenyl-aniline, brookite $(TiO_2)_{n\,=,\,8\,68,}$ clusters, and the dyes absorbed on the clusters. The results suggest that the absorption of dye molecules on TiO_2 brookite cluster improves its spectra responsivity in the UV region and makes it possible to absorb over the whole spectra range, that is, the UV, visible, and near-infrared region of the solar spectrum. Our findings on the adsorption energy revealed stable grafting of the polyenediphenyl-aniline dyes on the surface of the TiO_2 brookite clusters with

	HOMO (eV)	LUMO (eV)	Fermi level	GAP (eV)
D5	−4.91	−3.59	−4.25	1.32
D7	−4.81	−3.83	−4.27	0.98
D9	−4.72	−3.64	−4.33	1.08
D11	−4.77	−3.92	−4.27	0.85
$(TiO_2)_8$	−6.92	−4.62	−5.75	2.26
D5@$(TiO_2)_8$	−5.09	−4.40	−4.76	0.69
D7@$(TiO_2)_8$	−5.06	−4.39	−4.72	0.67
D9@$(TiO_2)_8$	−4.94	−4.43	−4.64	0.51
D11@$(TiO_2)_8$	−4.73	−4.19	−4.46	0.54

Table 3.
HOMO, LUMO, and HOMO_LUMO GAP energy levels.

D11 dyes demonstrating more grafting on both clusters $(TiO_2)_{n=,\,8\,68}$. The analyses of the isodensity surfaces of the key molecular orbital, electronic TDOS, and PDOS and HOMO, LUMO energy gap also showed new molecular orbitals emanating from the dye molecules into the bandgap of TiO_2 upon absorption. Due to interactions of the electronic states between the orbitals of the TiO_2 and the adsorbed dye molecules, suggesting good electron injection kinetics from the dyes occupied donor level to TiO_2 brookite clusters unoccupied acceptor level. Generally, our findings suggest that TiO_2 brookite semiconductor and the corresponding polyenediphenyl-aniline dyes could perform well as photoanode material with promising potential for higher photocurrents density and open-circuit voltage and enhanced efficiency of DSSCs.

Acknowledgements

We would also like thank the University of Venda, Centre for High performance Computing (CHPC), South Africa, and Centre for Interactive Materials and Bioinspired Technology, Albert Ludwig's University Freiburg in Germany for their computing facilities and the support to carry out this research.

Conflicts of interest

The authors declare that they have no known competing financial interests or personal relationships that could have appeared to influence the work reported in this paper.

DOI: http://dx.doi.org/10.5772/intechopen.1005450

Author details

Ife Elegbeleye[1,2*], Eric Maluta[1,3], Regina Maphanga[3,4], Michael Walter[2] and Oliver Brügner[2]

1 Department of Physics, University of Venda, Thohoyandou, South Africa

2 Freiburg Centre for Interactive and Bioinspired Technology, Freiburg, Germany

3 National Institute for Theoretical Physics (NIThePP), Gauteng, South Africa

4 Council for Science and Industrial Research, Pretoria, South Africa

*Address all correspondence to: ifelove778@gmail.com

References

[1] Mozhgan H, Zahra R. A review on flexible dye-sensitized solar cells as new sustainable energy resources. Pigment and Resin Technology. 2023;**52**:310-320. DOI: 10.1108/prt-01-2022-0010

[2] Abodunrin TJ, Obafemi O, Boyo AO, Adebayo TA, Jimoh R. The effect of electrolyte on dye sensitized solar cells using natural dye from mango (*M. Indica* L.) leaf as sensitizer. Advances in Material Physics and Chemistry. 2015;**5**:205-213. DOI: 10.4236/ampc.2015.56021

[3] Elegbeleye IF, Maluta NE, Maphanga RR. Density functional theory study of optical and electronic properties of $(TiO_2)_{n=5,8,68}$ clusters for application in solar cells. Molecules. 2019;**26**:1-19. DOI: 10.3390/molecules26040955

[4] Tong Z, Shang PG. The stability, electronic structure, and optical property of TiO_2 polymorphs. Journal of Physical Chemistry C. 2014;**118**:11385-11396. DOI: 10.1021/jp412462m

[5] Hao Y, Jia L, Gang Z, Sum WC, Hongda D, Lin G, et al. First principles study of ruthenium(ii) sensitizer adsorption on anatase TiO2 (001) surface. RSC Advances. 2015;**5**:60230-60236. DOI: 10.1039/C5RA06743J

[6] Mohammad KN, Filippo DA, Simona F, Annabella S, Guido V, Paul L, et al. Combined experimental and DFT-TDDFT computational study of photoelectrochemical cell ruthenium sensitizers. Journal of American Chemical Society. 2005;**127**:16835-16847. DOI: 10.1021/ja052467l

[7] Liyuan H, Ashraful I, Han C, Chandrasekharam M, Barreddi C, Shufang Z, et al. High efficient dye sensitized solar cell with novel co-adsorbent. Energy and Environmental Science. 2012;**5**:6057-6060. DOI: 10.1039/C2EE03418B

[8] Lu LL, Eric WGD. Porphyrin-sensitized solar cells. Chemical Society Reviews. 2013;**42**:291-304. DOI: 10.1039/C2CS35257E

[9] Boschloo G, Marinado T, Nonomura K, Edvinsson T, Agrios AG, Hagberg DP, et al. A comparative study of a polyene-diphenylaniline dye and $Ru(dcbpy)_2(NCS)_2$ in electrolyte-based and solid-state dye-sensitized solar cells. Thin Solid Films. 2008;**516**:7214. DOI: 10.1016/j.tsf.2007.12.035

[10] Daibin K, Pascal C, Shaik MZ, Daniel PH, Karl MK, Licheng S, et al. Stable dye-sensitized solar cells based on organic chromophores and ionic liquid electrolyte. Solar Energy. 2011;**85**:1189-1194. DOI: 10.1016/j.solener.2011.02.025

[11] Beltran A, Gracia L, Andres J. Density functional theory study of the brookite surfaces and phase transitions between natural titania polymorphs. Journal of Physical Chemistry B. 2006;**110**:23417-23423. DOI: 10.1021/jp0643000

[12] Maurizio A, Marianna B, Agatino DP, Leonardo P. Preparation and photoactivity of nanostructured anatase, rutile and brookite TiO_2 thin films. Chemical Communications. 2006;**47**:4943-4945. DOI: 10.1039/B612172A

[13] Damien D, Ilias B, Khalil A. Tailored preparation methods of TiO_2 anatase, rutile, brookite: Mechanism of formation and electrochemical properties. Chemical Materials. 2010;**22**:1173-1179. DOI: 10.1021/cm902613h

[14] Tarek AK, Armin F, Lars R, Ralf D, Detlef WB. Tailored titanium dioxide nanomaterials: Anatase nanoparticles and brookite nanorods as highly active photocatalysts. Chemical Materials. 2010;**22**:2050-2060. DOI: 10.1021/cm903472p

[15] Ken O, Bin L, Jin Z, Kenneth DJ, Jinlong Y, Hrvoje P, et al. Wet electrons at the $H_2O/TiO_2(110)$ surface. Science. 2005;**308**:1154-1158. DOI: 10.1126/science.1109366

[16] Zallen R, Moret MP. The optical absorption edge of brookite TiO_2. Solid State Communications. 2006;**137**:154-157. DOI: 10.1016/j.ssc.2005.10.024

[17] Pourjafari D, Reyes-Coronado D, Vega-Poot A, Escalante R, Kirkconnell-Reyes D, García-Rodríguez R, et al. Brookite-based dye-sensitized solar cells: Influence of morphology and surface chemistry on cell performance. Journal of Physical Chemistry C. 2018;**122**:14277-14288. DOI: 10.1021/acs.jpcc.8b02384

[18] Takayuki B, Ami H, Naoya A, Chika TY, Yutaka O. Hydrothermal synthesis of highly pure brookite-type titanium oxide powder from aqueous sols of titanate nanosheets. Advances Powder Technology. 2021;**32**:3601-3609. DOI: 10.1016/j.apt.2021.08.014

[19] Huy HD, Thi KCT, Thi DTU, Nguyen TD, Duc DN, Thu HT, et al. Controllable fabrication of photocatalytic TiO_2 brookite thin film by 3D-printing approach for dyes decomposition. Journal of Water Process Engineering. 2021;**43**:102319-1-10. DOI: 10.1016/j.jwpe.2021.102319

[20] Tingxin P, Jinlei X, Rong C. A novel multilayer brookite TiO_2 electrode for improved performance of pure brookite-based dye sensitized solar cells. Chemical Physics Letters. 2020;**738**:136902-1-6. DOI: 10.1016/j.cplett.2019.136902

[21] Gurenko VE, Popkov VI. Hydrothermal-assisted synthesis of sponge-like brookite for pseudo-fenton decomposition of crystal violet under UV–light. Nano-Structures and Nano-Objects. 2021;**28**(100801):1-6. DOI: 10.1016/j.nanoso.2021.100801

[22] Ask HL, Mortensen JJ, Jakob B, Ivano EC, Rune C, Marcin D, et al. The atomic simulation environment—A python library for working with atoms. Journal of Physics and Condensed Matter. 2017;**29**:1-59. DOI: 10.1088/1361-648X/aa680e

[23] Mortensen JJ, Lars BH, Karsten WJ. Real-space grid implementation of the projector augmented wave method. Physical. Review B. 2005;**71**:035109-1-11. DOI: 10.1103/PhysRevB.71.035109

[24] Enkovaara J, Rostgaard C, Mortensen JJ, Chen J, Dułak M, Ferrighi L, et al. Electronic structure calculations with GPAW: A real-space implementation of the projector augmented-wave method. Journal of Physics and Condensed Matter. 2010;**22**:253202-1-24. DOI: 10.1088/0953-8984/22/25/253202

[25] Perdew JP, Kieron B, Matthias E. Generalized gradient approximation made simple. Review Letters. 1996;**77**:3865-3868. DOI: 10.1103/PhysRevLett.77.3865

[26] Marcus DH, Donald EC, David CL, Tim V, Eva Z, Geoffrey RH. Avogadro: An advanced semantic chemical editor, visualization, and analysis platform. Journal of Chemical Information. 2012;**4**:1-17. DOI: 10.1186/1758-2946-4-17

[27] Mark EC. Time-dependent density functional response theory for molecules

in: Recent advances in density functional methods. Recent Advances in DFT Methods Workshop. 1995;**1**:155. DOI: 10.1142/9789812830586_0005

[28] Michael W, Hannu H, Lauri L, Martti P, Jussi E, Carsten R, et al. Time-dependent density-functional theory in the projector augmented-wave method. The Journal of Chemical Physics. 2008;**128**:244101-1-10. DOI: 10.1063/1.2943138

[29] Frisch MJ, Trucks GW, Schlegel HB, Scuseria GE, Robb MA, Cheeseman JR, et al. Gaussian 09, Revision B.01. Wallingford: Gaussian Inc.; 2010

[30] Becke AD. Density-functional exchange-energy approximation with correct asymptotic behavior. Physical Review A. 1988;**38**:3098-3100. DOI: 10.1103/PhysRevA.38.3098

[31] Chengteh L, Weitao Y, Robert GP. Development of the Colle-Salvetti correlation-energy formula into a functional of the electron density. Physical Review B. 1988;**37**:785-789. DOI 10.1103/PhysRevB.37.785

[32] Stewart JC, Matthew DS, Chris JP, Phil JH, Matt IP, Keith R, et al. First principles methods using CASTEP. Zeitschrift für Kristallographie—Crystalline Materials. 2005;**220**:567-570. DOI: 10.1524/zkri.220.5.567.65075

[33] Petre CIO, P, Fanica C, Marilena F, Mihai A. G. Density functional theory (DFT) study of coumarin-based dyes absorbed on TiO_2 nanoclusters—Applications to dye-sensitized solar cells. Materials. 2013;**6**:2372-2392. DOI: 10.3390/ma6062372

[34] Asif M, Salah UDK, Usman AR, Mudassir HT. Red shifting of absorption maxima of phenothiazine-based dyes by incorporating electron-deficient thiadiazole derivatives as π-spacer. Arabian Journal Chemistry. 2019;**12**:1447-1453. DOI: 10.1016/j.arabjc.2014.11.007

[35] Chiara A, Edoardo M, Mariachiara P, Enrico R, Filippo DA. Adsorption of organic dyes on TiO2 surfaces I,n dye-sensitized solar cells: Interplay of theory and experiment. Physical Chemistry Chemical Physics. 2012;**14**:15963-15974. DOI: 10.1039/C2CP43006A

[36] Avinash LP, Ramesh CK, Bhanuprakash K. Adsorption of croconate dyes on TiO_2 anatase (101) surface: A periodic DFT study to understand the binding of diketo groups. Journal of Chemical Science. 2012;**124**:301-310. DOI: 10.1007/s12039-012-0229-1

[37] Mariachiara P, Filippo DA. Computational modelling of TiO_2 surfaces sensitized by organic dyes with different anchoring groups: Adsorption modes, electronic structure and implication for electron injection/recombination. Physical Chemistry Chemical Physics. 2011;**14**:920-928. DOI: 10.1039/C1CP22663K

[38] Balaganapathi T, Kani Amuthan B, Vinoth S, Thilakan P. Synthesis, characterization and dye adsorption studies of porous brookite and mixed brookite with rutile TiO_2 using PEG assisted sol-gel synthesis. Material Research Bulletin. 2017;**19**:114-121. DOI: 10.1016/j.materresbull.2017.03.036

[39] Corneliu IO, Mihai AG. Structure and electronic properties of TiO_2 nanoclusters and dye–nanocluster systems appropriate to model hybrid photovoltaic or photocatalytic applications. Nanomaterials. 2019;**9**:1-31. DOI: 10.3390/nano9030357